Impact of Gore Cardioform Atrial Septal Defect Occluder on Atrial and Ventricular Electromechanics in a Pediatric Population

Biagio Castaldi, MD, PhD[a,*], Giuseppe Santoro, MD[b], Angela Di Candia, MD[a], Pietro Marchese, MD[b], Massimiliano Cantinotti, MD[b], Alessandra Pizzuto, MD[b], Silvia Scalera, MD[b], Silvia Garibaldi, MD[b], Jennifer Fumanelli, MD[a], Domenico Sirico, MD[a], and Giovanni Di Salvo, PhD, MD[a]

Transcatheter closure is the first-line treatment for ostium secundum atrial septal defect (ASD). The GORE Cardioform ASD Occluder (GCA) is potentially innovative compared with other self-centering devices. This study aimed to compare the mechanic changes in atrial and ventricular properties before and after GCA implantation. All consecutive patients aged <18 years who underwent isolated ASD closure with a single GCA device were enrolled from 2 centers. Echocardiography and electrocardiogram were performed the day before, 24 hours, and 6 months after ASD closure. Between January 2020 and February 2021, 70 pediatric patients with ASD were enrolled. The mean age was 7.9 ± 3.9 years, and the mean defect diameter was 17.1 ± 4.5 mm. Global longitudinal strain analysis showed no change in left ventricular longitudinal function (T0 −23.2 ± 2.8%, 24 hours −23.0 ± 2.8%, and 6 months −23.5 ± 2.7%). An early and transient reduction in longitudinal strain was detected in the basal septal segments (T0 −19.8 ± 3.3%, 24 hours −18.7 ± 3.6%, and 6 months −19.2 ± 3.4%), left atrium (T0 41.4 ± 15.3%, 29.2 ± 1.4%, and 39.0 ± 12.9%), and right ventricle (−27.6 ± 5.4%, −23.6 ± 5.0%, and −27.3 ± 4.6) 24 hours after closure, secondary to hemodynamic changes because of flow redirection after ASD closure. Six months after the procedure, only the left atrium showed a mild global longitudinal strain reduction because of the presence of the device within the septum. GCA device had no impact on global and regional ventricular function. Atrial mechanics were preserved, except for the segments covered by the device. This is the first device demonstrating no impact on the left and right ventricular mechanics, irrespective of the device size. **(Am J Cardiol 2024;211:259−267)**

Keywords: atrial septal defect, device, echocardiography, gore Cardioform device, interventional cardiology, speckle tracking

The first device for percutaneous closure of atrial septal defects (ASDs) was developed by King and Mills in 1972.[1] During the following years, the evolution of percutaneous implant devices has fitted within a path of innovation in the field of structural/congenital cardiology. The percutaneous approach represents the first-line treatment for ASD according to current guidelines,[2] as it shows higher benefits in terms of cost-effectiveness compared with the surgical one. Despite rare, erosion after Amplatzer septal occluder (ASO) (Abbott Amplatzer Septal Occluder) or ASO-like device implantation has been reported,[3] resulting in hemodynamic instability and need for surgical removal (incidence 0.1% to 0.3%).[5] Furthermore, several studies evaluated the impact of ASD devices on cardiac mechanics, showing a possible device negative impact on atrial function[6,7] and left ventricular (LV) basal-midwall segment deformation properties.[8] Similar studies found a correlation between device size and the magnitude of the speckle tracking parameter changes.[9] ASO or ASO-like devices are currently the most common devices used in the cath lab because of the ease of use and availability in a wide size range (4 to 38 to 42 mm).

Differently, GORE devices are made of a nitinol wire frame with a flower's petals shape, entirely covered with an expanded polytetrafluoroethylene membrane. Ideally, this design should reduce the risk of erosion secondary to the metal wires' interaction with the surrounding structures. In contrast, the softness of this device seems to facilitate prosthesis wire frame fractures (WFFs). The latter are relatively frequent in gore septal occluder (GSO) devices, accounting for up to 35% of the devices screened when routinely explored by fluoroscopy.[10,11] However, device removal is not recommended in the case of WFF because this event does not impact the device's function and stability, and the reports of complications are anecdotal.[12]

[a]Pediatric Cardiology Unit, Department of Women's and Children's Health, Univesity of Padua, Italy; and [b]Pediatric Cardiology Unit, Fondazione Toscana Gabriele Monasterio, Massa, Italy. Manuscript received August 24, 2023; revised manuscript received and accepted November 11, 2023.

Funding: none.

See page 266 for Declaration of Competing Interest.

*Corresponding author.

E-mail address: biagio.castaldi@unipd.it (B. Castaldi).

https://doi.org/10.1016/j.amjcard.2023.11.033

The GORE Cardioform ASD Occluder device (GCA, WL Gore & Associates, Flagstaff, Arizona) was designed with a self-centering mechanism to exploit the advantages of the versatile structure of the GSO device and allow the closure of a wider range of ASD sizes. GCA device recently received the Food and Drug Association (May 2018) and Conformite Europeenne (October 2019) marks and has been launched on the European market in January 2020.

This study aimed to evaluate atrial and ventricular electromechanic remodeling after ASD closure using a GCA device in a pediatric cohort. Available literature data about ASO or ASO-like devices or surgically closed ASD were used for comparison.

Methods

This is a single-arm prospective nonrandomized multicenter study conducted at the Pediatric Cardiology Unit of the University of Padua (Italy) and at the Pediatric Cardiology and ACHD Unit of the Ospedale del Cuore "G. Pasquinucci" in Massa (Italy). Pediatric patients with isolated, hemodynamically significant ostium secundum ASD scheduled for percutaneous closure between January 2020 and February 2021 were enrolled. Patients with genetic syndromes and significant cardiac or extracardiac co-morbidities were excluded. Indication for ASD closure was given in the presence of right ventricle volume overload on 2-dimensional (2D)-transthoracic echocardiography (TTE) evaluation (right ventricular [RV] end-diastolic diameter *Z* score >2; QP/QS >1.5, confirmed by invasive hemodynamic study; or RV end-diastolic diameter to LV end-diastolic diameter ratio >0.7). ASDs were considered "complex" in case of one or more deficient rims (<5 mm) except for aortic rim, aneurysmal, or multifenestrated (MF) septum or in case of the ASD diameter/patient's body weight ratio (ASD/BW) >1.2.

The study protocol complies with ethics guidelines according to the 1975 Declaration of Helsinki. The University of Padua Institutional Research Board approved this study (project code AOP2076).

The study end points were: (1) immediate procedural outcome, including the implantation rate and safety (adverse cardiac or extracardiac events and device embolization or unplanned rescue surgical treatment), complete closure of ASD, and short to medium-term clinical safety (free from cardiac or extracardiac adverse events) at 24 hours and 6 months after the procedure; and (2) changes in electromechanic properties by electrocardiogram (ECG), TTE, and 2D-speckle tracking strain analysis (S) were evaluated at baseline (T0), 24 hours (T24h), and 6 months (T6m) after the procedure.

At the admission to the Cardiology Unit (T0) a physical examination, routine blood tests, chest x-ray, ECG, TTE, and 2D-speckle tracking echocardiography (STE) were performed. Informed consent to the procedure was collected from the parents.

The interventional procedure was performed under general anesthesia with fluoroscopic guidance and transesophageal echocardiography. Measurement of the ASD diameter was obtained by static or dynamic sizing based on the operator preference. The device size was chosen based on the manufacturer's indications.[13] In the case of multiple ASDs, each of the significant defects was explored with a sizing balloon. Procedure and fluoroscopy times, radiation dose data (dose-area product), procedural complications, ECG early changes, adequate positioning of the device, and the presence of residual shunts were evaluated.

ECG, TTE, and STE were repeated at T24h and T6m. In addition, a 24-hour ECG Holter monitoring was performed 1 and 6 months after the procedure.

An adverse event was any complication that required previously unplanned cardiac or extracardiac treatment, unplanned hospitalization, or any medical problem involving long-term effects or requiring long-term treatment. Whenever possible, fluoroscopy was performed at 6 months to assess the presence of WFFs.

A Vivid E9 echocardiograph (GE Vingmed Ultrasound AS, Horten, Norway) with a 5 or 6-MHz probe was used for echocardiographic data collection. Conventional function parameters were collected: LV and RV diameters (M-mode from parasternal short-axis view); atrial septal length from subcostal left oblique view and from apical chambers view, we reported the longest one; LV ejection fraction calculated according to the Simpson biplane method; RV systolic function parameters (tricuspid annulus peak systolic excursion and S' systolic velocity peak from the tissue Doppler); LV diastolic function parameters (early diastole -E- velocity peak, atrial contraction -A- velocity peak and E/A ratio from the mitral valve inflow pattern; and E/E' ratio, where E′ was the average between lateral E′ and medial E' of the mitral annulus tissue Doppler spectrum).

Residual atrial shunts were classified as negligible (color Doppler jet ≤1 mm), mild (color Doppler jet ≤2 mm), moderate (color Doppler jet 2 to 4 mm), and severe (color Doppler jet ≥4 mm).

Atrial and ventricular longitudinal strain (L-S) analysis was performed on images saved in cine-loop format and analyzed offline using Echopac v12 software (GE, Echopac, Horten, Norway).

The LV L-S was assessed from the apical 4-, 3- and 2-chamber views. The RV, right atrium (RA), and left atrium (LA) L-S were assessed from the apical 4-chamber view. For the RA and RV L-S analysis, the septal segments were excluded (FW-RV=free wall right ventricle).[14,15] STE analysis was performed following current European Association of Cardiovascular Imaging recommendations.[14]

A standard 12-lead ECG was recorded at a rate of 25 mm/s and a calibration of 1 mV/cm for all the patients at the baseline. ECG was digitally stored. Thus, we were able to change appropriately the speed scale for postprocessing. P wave, PR interval, QRS amplitude, QRS, and QTc dispersion were manually measured using ComPacs software by 2 experienced operators, blinded on the clinical features of the patients. Parameters were recorded in all the leads available. (1) P wave: defined as the interval between the onset (junction of the isoelectric line at the beginning of the P wave deflection) to the offset (junction between the end of the P wave and the isoelectric line) of the P wave, (2) P wave dispersion (P dis=P max−P min) was calculated using these values, (3) PR interval: defined as the interval between the beginning of the P wave and the beginning of the QRS complex, (4) QRS voltage: defined as the

amplitude measured from the nadir of the QRS complex to its peak, (5) QRS duration: defined as the maximum QRS duration in any lead from the first to the last sharp vector crossing the isoelectric line, (6) QT interval: defined as the interval between the beginning of the QRS complex and the end of the T wave. QTc dispersion was defined as the difference between the maximum and minimum QTc intervals that could be measured in any of the 12 ECG leads but preferably in C2 or V5 lead. We calculated QTc using Bazzett's method. Heart rate was <100 beats/min in all the patients, so Friedericia correction was not necessary.

Statistical analysis

Statistical analysis was performed using the Statistical Package for the Social Sciences version 27.0 (SPSS Software, IBM, Chicago, Illinois). Continuous data was summarized by mean ± SD. The normal distribution of the variables was verified using the Kolmogorov−Smirnov test. Categoric variables are presented as absolute numbers and percentages. In the case of not-normal distribution, data were expressed in interquartile ranges. Comparisons between groups were made using the Student's *t* test for unpaired data. Comparison between different follow-up phases was performed using Wilcoxon's Test. Correlation between continuous data was performed using Spearman's test. Correlation between categoric data was performed using Pearson's test. The comparison between ≥3 groups of variables was performed using a one-way analysis of variance and post hoc Bonferroni Test (normal distribution) or by Kruskall−Wallis test (not-normal distribution) when appropriate. The null hypothesis was rejected for $p < 0.05$.

Results

Between January 2020 and February 2021, 70 consecutive pediatric patients underwent percutaneous closure of hemodynamically significant ASD using the GCA device. Demographic data are summarized in Table 1. The mean age was 8.4 ± 3.9 years. No significantly different characteristics were found in the subjects enrolled by the 2 centers. One patient had an aortic coarctation surgically corrected at birth without residual stenosis; a second patient showed a tiny ventricular septal defect with no significant QP/QS after percutaneous ASD closure. None of the patients had significant extracardiac co-morbidities or associated residual cardiac malformations or ventricular dysfunction.

ASD anatomical features, hemodynamic, and procedural data are listed in Table 1. The mean defect diameter was 17.1 ± 4.5 mm, and Qp/Qs was 1.7 ± 0.6. Thirty-eight patients (54.3%) had complex ASD because of a deficient rim except for aortic rim (deficient posterior rim n = 6, deficient posterior-inferior rim n = 7, and deficient superior cava rim n = 1; 12 patients in total), a MF atrial septum, fossa ovalis aneurysm (n = 21), and/or ASD/ BW >1.2 (n = 12). Nine patients had a deficient aortic rim. Nineteen patients (27%) had surgical indications for ASD closure because of a deficient posterior-inferior rim or ASD/ BW>1.2. The device was successfully implanted in 69 of 70 cases (98.6%) and in 64 (91.4%) at the first attempt. In 7 cases (10%), the device was oversized to cover the entire septal aneurysm, had close MF defects, or achieved greater stability on the deficient rim(s).

Table 1
Demographic data, anatomical features, and hemodynamic data. In case of multiple atrial septal defects, the diameter of the main defect was reported

Patients n°	70
Female n° (%)	46 (66)
Age (years)	7.9±3.9
Height (cm)	127.4±18.7
Weight (kg)	29.6±15.3
BSA (m2)	1.0±0.3
ASD size^ (mm)	17.1±4.5
ASD/BW (mm/kg)	0.7±0.3
Septal length (mm)	40.0±5.5
Device/Atrial septal length (mm/mm)	0.83±0.11
QP/QS	1.7±0.6
Mean pulmonary artery pressure (PAP, mmHg)	18.4±3.3
Total procedure time (min)	53.3 ±28.3
Fluoroscopy time (min)	10.1±6.6
Dose-Area Product (Gy*cm2)	12.1±10.2
Complex ASD n° (%)	38 (54)
- ASD diameter to body weight ratio >1.2	12 (17)
- Multi-fenestrated ASD and/or septal aneurysm	21 (30)
- Deficient aortic rim (<5,5 mm)	9 (13)
- Deficient posterior rim	6 (9)
- Deficient posterior-inferior rim	7 (10)
- Deficient superior caval rim	1 (1)
Implanted devices n° (%)	
- 27 mm	14 (20)
- 32 mm	31 (44)
- 37 mm	15 (21)
- 44 mm	10 (14)
Oversized devices n° (%)	7 (10)
Serious adverse events n° (%)	6 (9)
- device embolization	1 (1)
- clinically significant new arrhythmia	4 (6)
- pericardial effusion	1 (1)

ASD = atrial septal defect; BSA = body surface area; BW = body weight.

WFFs were investigated in 56% of patients at T6m; 38.5% had one or more wire frame fractures. None of them had fracture-related adverse events throughout the follow-up.

A complete ASD closure was achieved in 60 of 70 cases (85.7%) at T24h. Residual shunts have always been negligible or intraprosthetic. No residual shunts or adverse cardiovascular events were reported in any of the patients at T6m.

Six major adverse events were reported (8.6%). Early device embolization was seen in a 24 kg child with a 24 mm ASD once awake from sedation after implantation of a 44-mm device (single attempt) and required emergent cardiac surgery. Four cases of arrhythmia were reported: a case of variable atrioventricular block after closure of a 22 mm ASD with a 44-mm device, resolved spontaneously; a case of second-degree atrioventricular block occurred 24 hours after the implantation of a 37 mm GCA in a 22 mm ASD and regressed after steroid therapy; 2 cases of sustained supraventricular tachycardia responsive to antiarrhythmic therapy (β blocker), in a case of 18 mm ASD closed with a 37-mm device, and a 22 mm ASD closed with

44-mm device. Finally, a case of pericardial effusion treated with Ibuprofen was experienced by a 16 kg child with a 20 mm ASD closed with a 37 mm prosthesis.

Minor early adverse events were also recorded in 3 patients (4%): a case of vascular access bleeding resolved with manual compression; a case of hypersensitivity reaction related to acetylsalicylic acid administration during the procedure; and a case of mild laryngeal edema secondary to intubation, treated with antihistaminic and steroid therapy.

Standard echocardiographic data are listed in Table 2. A significant reduction in the right chamber sizes was observed 24 hours after the procedure (RV end-diastolic diameter and RA end-systolic volume, p <0.01). Similarly, a relative reduction in the RV longitudinal systolic function indexes was also observed (tricuspid annulus peak systolic excursion and RV s′, p <0.01 in both cases) despite their values remaining in the normal range.

Left chamber remodeling was more evident at the 6-month follow-up, reporting an increase in the LA volume (p <0.01), together with an increase in LV diameters (p <0.001), LV end-diastolic and end-systolic volumes (p <0.001), and LV mass (p <0.001), with comparable LV wall thickness.

STE data are summarized in Figure 1 and Table 3. At T24h, a negative impact on left atrial function was observed (LA L-S from 41.4 ± 15.3% at T0 to 29.2 ± 11.4% at T24h, p <0.001). It was more evident in the septal segments because of the presence of the device within the septum. A gradual recovery of LA-LS was reported at T6m (39.0 ± 12.9%, p = 0.02 vs T24h).

The device showed no impact on the LV global L-S (T0: −23.2 ± 2.8%; T6m: −23.0 ± 2.7). Analyzing single segments, a transient significant reduction of the LV basal posterior septal and basal anterior-septal segments L-S at T24h evaluation was found, with recovery at T6m (basal posterior septal: T0 −19.8 ± 3.3%, T24h −18.7 ± 3.6%, p = 0.04, and T6m −19.2 ± 3.4%, p = NS vs T0; basal anterior-septal: −20.8 ± 4.6%, −19.5 ± 4.4%, and −20.1 ± 4.3%, respectively, p = 0.03 at 24 hours vs T0).

A transient reduction of the RV L-S was observed at T24h, with recovery at T6m (−27.6±5.4%; −23.6 ± 5.0%, p <0.001 vs T0; −27.3 ± 4.6%).

Basrd on ECG data, the baseline mean P wave dispersion decreased from 40 ± 15 ms (baseline) to 30 ± 13 ms at 6 months (p <0.001). QTc significantly improved at 6 months from the procedure (from 405.0 ± 19.1 to 397.2 ± 14.5 ms, p = 0.01). QTc dispersion significantly decreased (from 40.9 ± 13.0 to 28.0 ± 18.2, p <0.001) at 6 months from the procedure.

Preoperative P wave duration and P wave dispersion correlated with T0 RA strain (R = −0.43, p = 0.01 and R = 0.42, p = 0.01, respectively) and LA strain (R = −0.36, p = 0.03; R = −0.34, p = 0.04). At 6 months, no correlation was found between P wave dispersion and RA and LA strain.

QTc wave duration and QTc wave dispersion did not show any correlation with RV or LV strain value before and after ASD closure.

Defect size correlated with T0 P wave duration (R = 0.37, p = 0.02) and with P wave dispersion (R = 0.29, p = 0.04). No correlation was found between P and QTc waves duration and dispersion and device size or device size-to-atrial septal length ratio.

By analyzing speckle tracking data for device size (Table 4), no difference was found in L-S between T0 and T6m, irrespective of device size. A transient impairment of LA strain was found in all the subgroups 24 hours after the procedure. Further, we explored the correlation between device size-to-weight ratio and strain parameters to consider the impact of the device on small patients and small atria. We find a negative correlation between device size-to-weight ratio and device size-to-atrial septal length ratio with LA strain 24 hours after the procedure (R^2 = 0.33, p <0.001; R^2 = 0.20, p = 0.01), but not at T6m (Figure 2).

In addition, we analyzed simple ASD vs complex ASD separately. As different complex characteristics can coexist in the same patient, we divided complex cases into 2 groups: MF and deficient rims group (Figure 3, Table 5). No significant differences in deformation imaging values were found between complex and simple ASD, except for LA strain at T24h, with LA L-S values at T24h significantly lower in the complex ASD group rather than in the not-complex one (33.0 ± 12.9 vs 26.5 ± 9.9, p = 0.03).

Analyzing single characteristics within the complex group, the deficient rims group appears to have a transient reduction of L-S values at T24h, with complete recovery at T6m.

Table 2
Standard echocardiographic data

	T 0	T 24 h	T 6 months
LVEDD (mm)	34.5±6.8	36.0±5.7*	39.9±5.3*
LVESD (mm)	21.5±3.8	21.6±3.9*	25.0±4.5*
BP-LVEDV (mL)	47.1±20.1	48.7±19.7*	56.9±21.7*
BP- LVESV (mL)	16.1±7.1	17.2±7.4*	20.5±8.6*
BP- LVEF (%)	70±7	65±6	64±7
RVEDD (mm)	23.5±5.5	20.0±4.4*	18.5±4.3*
TAPSE	23.6±3.9	21±4.3*	21.6±4.5
RV-S'	14.4±2.0	12.6±2.2*	13.3±2.4
E/A	1.7±0.4	1.9±0.6*	1.9±0.5
E/E' Avg	6.1±1.4	8.0±2.5*	6.8±2.2*

* p<0,05 compared to T0 (paired data T-Student test).

BP-LVEDV = biplane left ventricular end diastolic volume; BP-LVEF = biplane left ventricular ejection fraction; BP-LVESV = biplane left ventricular end systolic volume; E/A = mitral valve E wave A wave ratio; E/E' Avg = mitral valve E wave to mean E' TDI value ratio; LVEDD = left ventricular end diastolic diameter; LVESD = left ventricular end systolic diameter; RVEDD = right ventricular end diastolic diameter; RV-S' = right ventricular S' value; TAPSE = tricuspid annulus peak systolic excursion.

Discussion

Percutaneous ASD closure has been extensively compared with surgery in terms of efficacy,[15,16] electrical and/or mechanic heart chamber remodeling,[17,18] and early or late adverse events.[4,19–24] Thus, current guidelines recommend the interventional approach as the treatment of choice for ASD closure when technically feasible.[2]

Historically, ASD devices were clustered into 2 types: self-centering devices (ASO and similar) and not-self-

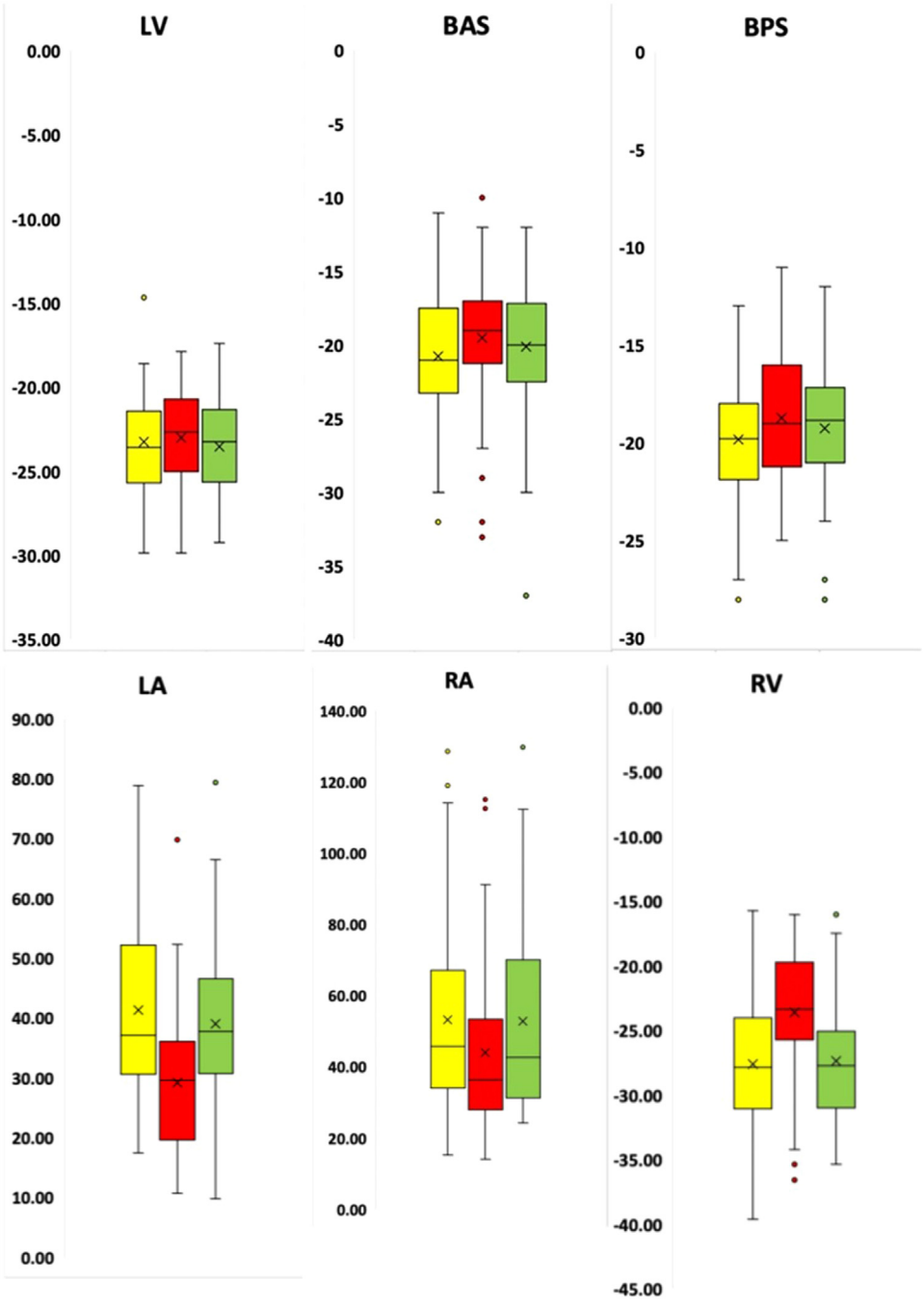

Figure 1. Box-plot analysis of global and segmental strain (in %) at T0 *(yellow boxes)*, T24h *(red boxes)*, and 6 m *(green boxes)*. There was a statistically significant reduction at 24 hours in BAS, BPS, LA, and RV, whereas no significant difference was found in the LV and RA. BAS = basal anterior septum; BPS = basal posterior septum.

Table 3
Global and segmental speckle tracking analysis (%)

	T 0	T 24 h	T 6 months
Left atrium	41.4 ± 15.3	29.2 ± 11.4*	39.0 ± 12.9*
Left ventricle	-23.2 ± 2.8	-23.0 ± 2.8	-23.5 ± 2.7
Basal ant. septum	-20.8 ± 4.6	-19.5 ± 4.4 *	-20.1 ± 4.3
Basal post. septum	-19.8 ± 3.3	-18.7 ± 3.6*	-19.2 ± 3.4
Right atrium	53.2 ±27.6	44.0 ± 23.8	52.8 ± 22.2
Right ventricle	-27.6 ± 5.4	-23.6 ± 5.0*	-27.3 ± 4.6

* p<0,05 compared to T0 (paired data T-Student test).

centering devices (GSO, Amplatzer Cribriform device and similar). GCA is a new device with an "adaptable waist." It represents a third cluster of devices, able to merge some features of both the groups previously mentioned: like ASO, GCA can be used to close large defects (up to 35 mm); like not-self-centering devices, it is softer and, after the release, spontaneously finds a central position on the septum, reducing the tension on the surrounding structures and the risk of erosion. Thus, this device widened the feasibility of percutaneous treatment in challenging anatomies (like facing rims deficiency) previously scheduled for

Table 4
Comparison of strain values (%) for each device sizes

	LV			LA			RV			RA		
	T0	T24h	T6m	T0	T24h	T6m	T0	T24h	T6m	T0	T24h	T6m
GCA 27	-21.6±3.0	-21.8±2.8	-21.7±1.1	50.5±12.7	42.4±11.5*	56.5±18.0	-30.5±6.3	-24.8±4.2*	-30.2±4.0	57.4±11.4	38.2±16.7*	58.4±17.6
GCA 32	-23.3±2.5	-22.3±1.9*	-23.2±2.8	43.8±15.9	31.3±9.9*	41.1±10.9	-28.0±5.0	-25.6±5.4	-28.7±3.5	68.4±34.8	52.3±24.0	55.7±24.3
GCA 37	-24.6±2.4	-24.0±1.7	-24.6±3.3	31.9±7.5	24.3±7.1*	35.6±13.2	-22.0±4.6	-21.2±3.6	-24.0±6.5	30.7±13.5	25.8±8.3	38.3±10.4
GCA 44	-23.3±2.8	-22.6±2.6	-22.6±2.5	32.4±7.0	17.6±5.2*	36.4±5.6	-26.7±4.6	-19.3±1.8*	-29.0±3.5	51.3±27.2	32.7±7.8	36.6±7.8

* p<0,05 compared to T0 (paired data T-Student test).
LA = left atrium, LV = left ventricle; RA = right atrium; RV = right ventricle.

surgical closure.[25] However, the deployment requires an adequate learning curve, and it can be poorly manipulated during the disks' conformation compared with ASO devices. In our population, despite the high rate of challenging settings, the GCA device showed high versatility and effectiveness, with fluoroscopy times, x-ray dose, efficacy, and safety rates compared with other devices.[9,26,27] The incidence of any complications in our population was 8.6%, compared with that reported in preliminary studies.[10,28]

The large gamma of devices available for ASD closure changed the approach to the procedure. In the past decades, the aim of the operator was just to effectively close the defect. Nowadays, the device's choice should take into account the best match between ASD anatomy and the device. Although percutaneous closure has been proved to be superior to surgery regarding the preservation of LV mechanics, the impact of devices on this subject is not negligible.[6–8,29]

This is the first study that investigates the remodeling and deformation of heart chambers in pediatric patients who underwent percutaneous closure using GCA devices. Our results confirmed a positive reverse remodeling using TTE after ASD closure, which agrees with the results obtained with other devices.[29] In addition, the impact on heart chamber mechanics using STE was just limited to atrial function because of the mere presence of the device on the atrial septum. In addition, device size had a transient impact on LA L-S, with a normalization at T6m (Figure 3). Our data showed preserved and unchanged global LV L-S values 6 months after the procedure. Similarly to LA, the impact on basal segments was limited to the first 24 hours. Most importantly, strain values remained unchanged irrespective of the device size, in contrast with similar studies performed on ASO devices, where larger devices (ASD size >15 mm) showed a heavier impact on LV deformation properties of basal segments.[9]

ECG parameters showed positive atrial and ventricular remodeling. P wave dispersion was associated with paroxysmal supraventricular arrhythmias in several medical or surgical settings.[30–33] In our patients, P wave and QTc dispersion progressively improved after ASD closure. We found a correlation between ASD size, atrial strain values, P wave duration, dispersion at T0, and normalization of electrical parameters at T6m. Interestingly, no correlation

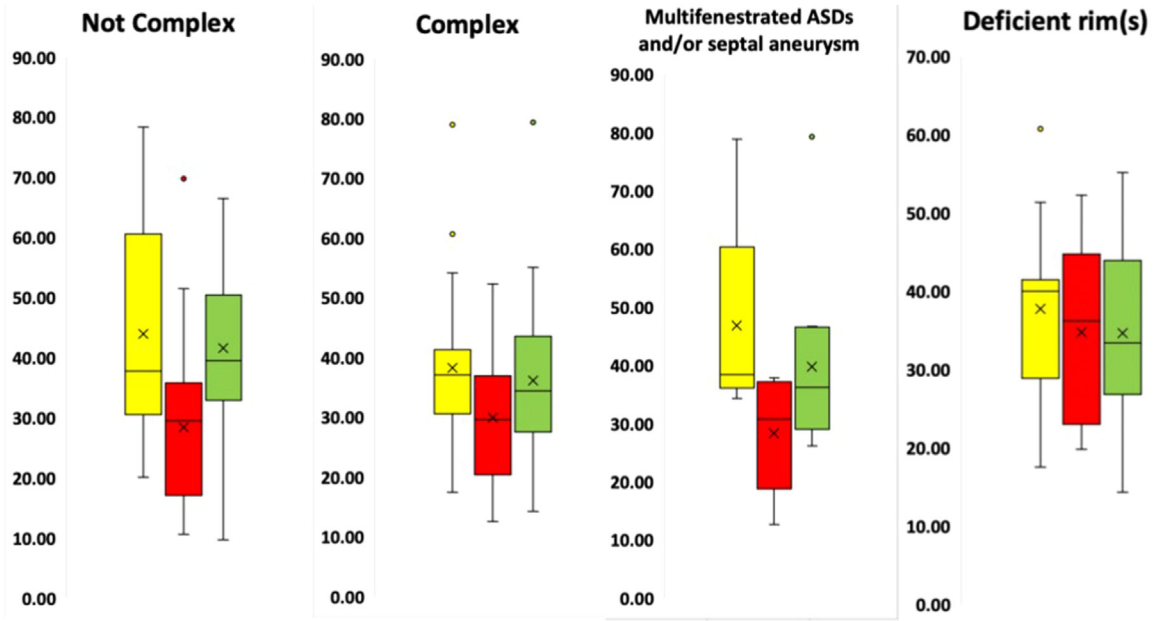

Figure 2. Correlation between LA strain (%) and device size corrected to patients' body weight ratio at 24 hours *(left)* and at 6 months *(right)*. There was a significant correlation between LA strain impairment and device size to body weight ratio at 24 hours (R^2 = 0.34, p <0.001), which was not confirmed at 6 months (R^2 = 0.036, p = 0.17).

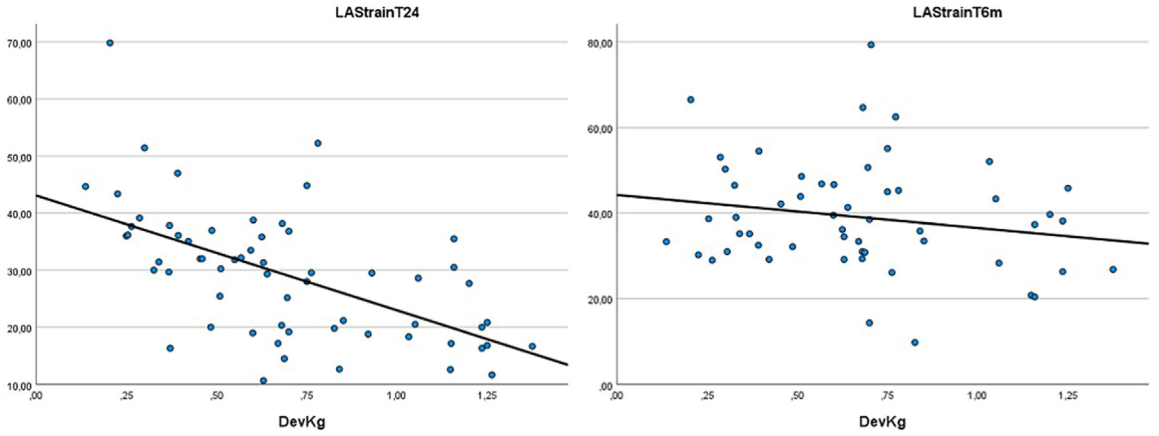

Figure 3. Differences in LA strain (in %) in different subgroups at T0 *(yellow boxes)*, T24h *(red boxes)*, and 6 months *(green boxes)*. There was a transient LA strain impairment 24 hours after the procedure in all the subgroups.

was found between P dispersion and device size. These data confirm and agree with STE the lower impact of GCA devices on atrial and ventricular mechanics.

There are conflicting data about electrical remodeling after percutaneous ASD closure. Santoro et al[31,32] showed a reduction of P wave duration and dispersion after device implantation. In contrast, Thilén et al[33] did not find any improvement after the device or surgical treatment. Compared with these studies, our cohort of patients was larger (70 vs 15 and 21 patients) and younger (mean age 8.4 vs 23 and 53 years). Our data confirm that an ASD closure in pediatric age can effectively prevent irreversible electrical remodeling, reducing the risk of arrhythmias in these patients. Kaya et al[33] studied a cohort of 112 patients (65 children and 47 adults) before and after percutaneous ASD closure. They demonstrated a reduction in P wave dispersion and QT dispersion. Unfortunately, the authors did not compare the impact of electrical mechanics in pediatric versus adult patients. In summary, our data confirm that, like with other ASD devices, percutaneous ASD closure in pediatric age warrants a reverse remodeling in atrial electromechanics.

WFFs are relatively common in Gore devices. The ASSURED trial[9] and a previous work of the authors of this manuscript reported an incidence of 36% of WFF in patients with ASD treated using GSO devices.[10] Similarly, WFF was found in 38.5% of our population detected by fluoroscopy. Despite the frequency of WFF, no device dysfunction or clinical sequelae were found at midterm follow-up. Currently, WFF is not considered a clinically relevant problem for this kind of device. In addition, no electromechanic impairment was demonstrated in these patients.

Based on our experience, the GCA device showed no impact on the LV longitudinal function, suggesting a higher adaptability to heart mechanics compared with other devices despite a comparable closure and complication rate.

This is a short-term follow-up study. No data are available on long-term follow-up because of the recent availability of this new device. Although the impact of wire frame fracture on a long-term follow-up is unknown, previous studies on Gore devices ensure the preserved device function in case of fracture. STE suffers from intra and interobserver variability. However, in our study, the speckle tracking was acceptable and reproducible, as already reported in other similar studies. This study was performed in 2 different centers. Thus, the image acquisition and postprocessing were performed by different operators.

In conclusion, GCA device has proved to be safe, highly versatile, and effective for ASD percutaneous closure. This study demonstrated that GCA had no impact on global and regional right and LV longitudinal function 6 months after implantation. Atrial mechanics were preserved, except for the segments covered by the device, with a tendency for

Table 5
Subgroup analysis (strain values, in %)

	Not Complex			Complex			MF or aneurismatic ASD			Deficient rim(s)		
	T0	T24h	T6m	T0	T24h	T6m	T0	T24h	T6m	T0	T24h	T6m
LA	44.0±16.6	33.1±12.5^	41.9±12.7	42.4±13.0	25.0±10.4^	35.1±10.2	46.8±17.3	33.3±4.7^	39.9±16.6	35.6±11.0	21.4±9.3*^	35.3±10.9
LV	-23.3±2.9	-22.7±2.3	-23.0±2.5	-23.1±2.7	-22.5±2.6	-23.6±3.0	-23.0±2.3	-22.0±3.0	-23.0±3.3	-23.1±2.9	-23.0±2.7	-23.2±2.8
BAS	-21.5±4.3	-20.6±4.0	-22.3±4.6	-23.5±6.3	-20.6±6.2^	-23.0±5.8	-22.0±3.4	-21.3±5.4	-23.8±3.7	-24.0±7.0	-20.6±6.2^	-23.1±6.4
BPS	-20.0±3.6	-19.1±2.8	-19.4±2.7	-19.4±3.0	-17.5±4.0	-19.5±3.2	-19.0±1.9	-19.2±3.4	-18.7±3.6	-19.5±3.4	-17.3±4.3^	-20.0±3.4
RA	49.2±27.8	45.7±27.3^	57.3±30.7	57.4±28.1	47.2±22.4^	55.5±19.0	54.7±11.6	52.9±21.9	60.4±21.1	58.4±32.2	40.8±20.3^	51.3±17.8
RV	-26.8±6.0	-23.9±5.0^	-27.5±5.1	-28.2±4.7	-23.9±4.6^	-28.6±3.2	-29.5±6.1	-23.7±4.6^	-28.9±3.2	-27.9±4.1	-23.2±5.0^	-28.3±3.5

* p-value <0.05 compared to not complex and multifenestrated ASDs. (ANOVA with post hoc Bonferroni analysis). ^p-value <0.05 compared to baseline (t-test paired data).

ASD = atrial septal defect; BAS = basal anterior septum; BPS = basal posterior septum; MF = multi-fenestrated; LA = left atrium, LV = left ventricle; RA = right atrium; RV = right ventricle.

global atrial function recovery at 6-month follow-up. Based on the data available in the literature, this was the first device to demonstrate no impact on the LV and RV mechanics, irrespective of the device size used.

Declaration of Competing Interest

Dr. Santoro is a proctor for WL Gore. The remaining authors have no competing interests to declare.

Data Availability

All relevant data were reported in the study. Further data can be obtained by sending a motivated request by mail to the corresponding author.

1. King TD, Thompson SL, Steiner C, Mills NL. Secundum atrial septal defect. Nonoperative closure during cardiac catheterization. *JAMA* 1976;235:2506–2509.
2. Baumgartner H, De Backer J, Babu-Narayan SV, Budts W, Chessa M, Diller GP, Lung B, Kluin J, Lang IM, Meijboom F, Moons P, Mulder BJM, Oechslin E, Roos-Hesselink JW, Schwerzmann M, Sondergaard L, Zeppenfeld K, ESC Scientific Document Group. 2020 ESC Guidelines for the management of adult congenital heart disease. *Eur Heart J* 2021;42:563–645. 3.
3. Amin Z, Hijazi ZM, Bass JL, Cheatham JP, Hellenbrand WE, Kleinman CS. Erosion of Amplatzer septal occluder device after closure of secundum atrial septal defects: review of registry of complications and recommendations to minimize future risk. *Catheter Cardiovasc Interv* 2004;63:496–502.
4. Turner DR, Owada CY, Sang CJ, Khan M, Lim DS. Closure of secundum atrial septal defects with the Amplatzer septal occluder: a prospective, multicenter, post-approval study. *Circ Cardiovasc Interv* 2017;10:e004212.
5. Abd El Rahman MY, Hui W, Timme J, Ewert P, Berger F, Dsebissowa F, Hetzer R, Lange PE, Abdul-Khaliq H. Analysis of atrial and ventricular performance by tissue Doppler imaging in patients with atrial septal defects before and after surgical and catheter closure. *Echocardiography* 2005;22:579–585.
6. Di Salvo G, Drago M, Pacileo G, Rea A, Carrozza M, Santoro G, Bigazzi MC, Caso P, Russo MG, Carminati M, Calabro' R. Atrial function after surgical and percutaneous closure of atrial septal defect: a strain rate imaging study. *J Am Soc Echocardiogr* 2005;18:930–933.
7. Di Salvo G, Drago M, Pacileo G, Carrozza M, Santoro G, Bigazzi MC, Caso P, Russo MG, Carminati M, Calabró R. Comparison of strain rate imaging for quantitative evaluation of regional left and right ventricular function after surgical versus percutaneous closure of atrial septal defect. *Am J Cardiol* 2005;96:299–302.
8. Castaldi B, Santoro G, Di Salvo G, Gaio G, Palladino MT, D'Aiello F, Iacono C, Pacileo G, Calabrò R, Russo MG. Impact of the Amplatzer atrial septal occluder device on left ventricular function in pediatric patients. *Pediatr Cardiol* 2013;34:1645–1651.
9. Sommer RJ, Love BA, Paolillo JA, Gray RG, Goldstein BH, Morgan GJ, Gillespie MJ, ASSURED Investigators. ASSURED clinical study: new GORE® CARDIOFORM ASD occluder for transcatheter closure of atrial septal defect. *Catheter Cardiovasc Interv* 2020;95:1285–1295.
10. Castaldi B, Cabrelle G, Padalino M, Vida V, Milanesi O, Di Salvo G. Percutaneous closure of patent foramen ovale and secundum atrial septal defects with the GORE CARDIOFORM septal occluder: incidence andImplications of device wire frame fracture. *Congenit Heart Dis* 2020;15:347–360.
11. Kumar P, Orford JL, Tobis JM. Two cases of pericardial tamponade due to nitinol wire fracture of a gore septal occluder. *Catheter Cardiovasc Interv* 2020;96:219–224.
12. GORE® CARDIOFORM ASD Occluder IFU. Gore. Available at: https://eifu.goremedical.com/. Accessed on December 6, 2023.
13. Badano LP, Kolias TJ, Muraru D, Abraham TP, Aurigemma G, Edvardsen T, D'Hooge J, Donal E, Fraser AG, Marwick T, Mertens L, Popescu BA, Sengupta PP, Lancellotti P, Thomas JD, Voigt JU. Industry representatives, Reviewers: This document was reviewed by members of the 2016–2018 EACVI Scientific Documents Committee. Standardization of left atrial, right ventricular, and right atrial deformation imaging using two-dimensional speckle tracking echocardiography: a consensus document of the EACVI/ASE/Industry Task Force to standardize deformation imaging. *Eur Heart J Cardiovasc Imaging* 2018;19:591–600.
14. Badano LP, Muraru D, Parati G, Haugaa K, Voigt JU. How to do right ventricular strain. *Eur Heart J Cardiovasc Imaging* 2020;21:825–827.
15. Du ZD, Hijazi ZM, Kleinman CS, Silverman NH, Larntz K, Amplatzer Investigators. Comparison between transcatheter and surgical closure of secundum atrial septal defect in children and adults: Results of a multicenter nonrandomized trial. *J Am Coll Cardiol* 2002;39:1836–1844.
16. Ooi YK, Kelleman M, Ehrlich A, Glanville M, Porter A, Kim D, Kogon B, Oster ME. Transcatheter versus surgical closure of atrial septal defects in children: a value comparison. *JACC Cardiovasc Interv* 2016;9:79–86.
17. Castaldi B, Vida VL, Argiolas A, Maschietto N, Cerutti A, Gregori D, Stellin G, Milanesi O. Late electrical and mechanical remodeling after atrial septal defect closure in children: surgical versus percutaneous approach. *Ann Thorac Surg* 2015;100:181–186.
18. Komar M, Przewłocki T, Olszowska M, Sobień B, Stępniewski J, Podolec J, Mleczko S, Tomkiewicz-Pająk L, Żmudka K, Podolec P. Conduction abnormality and arrhythmia after transcatheter closure of atrial septal defect. *Circ J* 2014;78:2415–2421.
19. Divekar A, Gaamangwe T, Shaikh N, Raabe M, Ducas J. Cardiac perforation after device closure of atrial septal defects with the Amplatzer septal occluder. *J Am Coll Cardiol* 2005;45:1213–1218.
20. Jalal Z, Hascoët S, Gronier C, Godart F, Mauri L, Dauphin C, Lefort B, Lachaud M, Piot D, Dinet ML, Levy Y, Fraisse A, Ovaert C, Pillois X, Lusson JR, Petit J, Baruteau AE, Thambo JB. Long-term outcomes after percutaneous closure of ostium secundum atrial septal defect in the young: a nationwide cohort study. *JACC Cardiovasc Interv* 2018;11:795–804.
21. Grohmann J, Wildberg C, Zartner P, Abu-Tair T, Tarusinov G, Kitzmüller E, Schmoor C, Stiller B, Kampmann C. Multicenter midterm follow-up results using the gore septal occluder for atrial septal defect closure in pediatric patients. *Catheter Cardiovasc Interv* 2017;89:E226–E232.
22. Gillespie MJ, Javois AJ, Moore P, Forbes T, Paolillo JA, Investigator Group GSO. Use of the GORE® CARDIOFORM Septal Occluder for percutaneous closure of secundum atrial septal defects: results of the multicenter U.S. IDE trial. *Catheter Cardiovasc Interv* 2020;95:1296–1304.
23. Moore J, Hegde S, El-Said H, Beekman R, Benson L, Bergersen L, Holzer R, Jenkins K, Ringel R, Rome J, Vincent R, Martin G. ACC IMPACT Steering Committee. Transcatheter device closure of atrial septal defects: a safety review. *JACC Cardiovasc Interv* 2013;6:433–442.
24. Butera G, Romagnoli E, Carminati M, Chessa M, Piazza L, Negura D, Giamberti A, Abella R, Pomè G, Condoluci C, Frigiola A. Treatment of isolated secundum atrial septal defects: impact of age and defect morphology in 1,013 consecutive patients. *Am Heart J* 2008;156:706–712.
25. Santoro G, Castaldi B, Cuman M, Di Candia A, Pizzuto A, Sirico D, Cantinotti M, Garibaldi S, Pak V, Di Salvo G. Trans-catheter atrial septal defect closure with the new GORE® Cardioform ASD occluder: first European experience. *Int J Cardiol* 2021;327:68–73.
26. de Hemptinne Q, Horlick EM, Osten MD, Millán X, Tadros VX, Pighi M, Gonzalez Barlatey F, Alnasser SM, Miró J, Asgar AW, Ibrahim R. Initial clinical experience with the GORE® CARDIOFORM ASD occluder for transcatheter atrial septal defect closure: ASD Closure with GORE® CARDIOFORM ASD Occluder. *Catheter Cardiovasc Interv* 2017;90:495–503.
27. Tanghöj G, Odermarsky M, Naumburg E, Liuba P. Early complications after percutaneous closure of atrial septal defect in infants with procedural weight less than 15 kg. *Pediatr Cardiol* 2017;38:255–263.
28. Menting ME, van den Bosch AE, McGhie JS, Cuypers JAAE, Witsenburg M, Geleijnse ML, Helbing WA, Roos-Hesselink JW. Ventricular myocardial deformation in adults after early surgical repair of atrial septal defect. *Eur Heart J Cardiovasc Imaging* 2015;16:549–557.
29. Xu Q, Sun L, Zhou W, Tang Y, Ding Y, Huang J, Wang H, Hou C, Lv H. Evaluation of right ventricular myocardial strains by speckle tracking echocardiography after percutaneous device closure of atrial septal defects in children. *Echocardiography* 2018;35:1183–1188.

30. Santoro G, Pascotto M, Sarubbi B, Cappelli Bigazzi M, Calvanese R, Iacono C, Pisacane C, Palladino MT, Pacileo G, Russo MG, Calabrò R. Early electrical and geometric changes after percutaneous closure of large atrial septal defect. *Am J Cardiol* 2004;93:876–880.
31. Santoro G, Pascotto M, Caputo S, Gaio G, Iacono C, Caso I, Sarubbi B, Carrozza M, Russo MG, Calabrò R. Short-term electrogeometric atrial remodelling after percutaneous atrial septal defect closure. *J Cardiovasc Med (Hagerstown)* 2008;9:789–793.
32. Thilén U, Carlson J, Platonov PG, Olsson SB. Atrial myocardial pathoelectrophysiology in adults with a secundum atrial septal defect is unaffected by closure of the defect. A study using high resolution signal-averaged orthogonal P-wave technique. *Int J Cardiol* 2009; 132:364–368.
33. Kaya MG, Baykan A, Dogan A, Inanc T, Gunebakmaz O, Dogdu O, Uzum K, Eryol NK, Narin N. Intermediate-term effects of transcatheter secundum atrial septal defect closure on cardiac remodeling in children and adults. *Pediatr Cardiol* 2010;31:474–482.